Lucia Plank et al.: Processing SELENE Differential VLBI Data, IVS 2012 General Meeting Proceedings, p.291–295
http://ivscc.gsfc.nasa.gov/publications/gm2012/plank.pdf

Processing SELENE Differential VLBI Data

Lucia Plank, Johannes Böhm, Matthias Madzak, Claudia Tierno Ros, Harald Schuh

Institute of Geodesy and Geophysics, Vienna University of Technology
Contact author: Lucia Plank, e-mail: `lucia.plank@tuwien.ac.at`

Abstract

The Japanese lunar mission SELENE was observed in differential VLBI (D-VLBI) mode with terrestrial VLBI antennas in Japan and overseas. We present our experience of processing D-VLBI data with the Vienna VLBI Software (VieVS). When processing D-VLBI data, many parameters (e.g. station coordinates or a priori spacecraft positions) have less influence on the computed time delay than in "normal" geodetic VLBI. For the SELENE data, this level of cancellation is determined empirically and presented for various parameters. With the atmosphere being identified as a possible source of remaining errors, the effects of the ionosphere, the wet troposphere, and of tropospheric turbulences were investigated more deeply. By estimating relative spacecraft positions of the SELENE satellites, the potential of spacecraft VLBI used for precise positioning is discussed.

1. SELENE

In the years 2007-2009 the Japanese Aerospace Exploration Agency (JAXA) flew a lunar project named Selenological and Engineering Explorer (SELENE). SELENE consisted of three satellites: the main orbiter named Kaguya and the two sub-satellites called Rstar and Vstar. During the mission, whenever the two sub-satellites were close together (with a separation angle $<0.56°$) and no other tracking was active, same-beam differential VLBI (D-VLBI) observations were performed. Up to eight VLBI telescopes at a time received the two signals from Rstar and Vstar in one antenna beam, without the need to switch between the sources. After correlation of the recorded signals, the measured quantity is the differential phase delay ($\Delta\tau$), representing the difference between the two VLBI delays of a baseline to the two sources.

$$\Delta\tau = \tau_{Rstar} - \tau_{Vstar} \tag{1}$$

According to [6], the nominal accuracy of the S-band differential phase delay is 3.44 ps rms, corresponding to $\sim$1 mm. For detailed information about the signal structure, the observation process, and the derivation of the observable we refer to further literature, e.g. [8]. With its sensitivity to the relative angular position of the satellites, D-VLBI is the perfect complement to the mainly used two-way tracking (with Doppler or range signals), which is only sensitive in the direction of the line of sight. Overall, the effort of including D-VLBI observations in the determination of the orbits of Rstar and Vstar improved the orbit consistency during the entire mission from several hundreds to several tens of meters [5].

1.1. Data

The VLBI tracking was done using the Japanese VERA (VLBI Exploration of Radio Astronomy) network, with stations in Iriki (IRI), Ishigaki (ISI), Mizusawa (MZW), and Ogasawara

(OGW). Additionally, there were also two international campaigns, complementing the network with antennas in Hobart, Australia (HOB); Urumqi, China (URQ); Shanghai, China (SHA); and Wettzell, Germany (WTZ). For our investigations we analyzed two datasets:

- October 2008, 17-22: IRI, ISI, MZW, OGW (Japanese)
- January 2008, 12-16: IRI, ISI, MZW, OGW, HOB, URQ, SHA, WTZ (intercontinental).

2. Processing

For the processing, the Vienna VLBI Software (VieVS) [1] was adopted for the ability to process D-VLBI data. This means that the delay model, commonly designed for observations to far distant and quasi-static quasars, had to be adopted for moving sources at finite distances. We implemented the formula given by Sekido and Fukushima (2006) [10] and verified its correct application through the comparison with the formulas given by Fukushima (1994) [3] and by Klioner (1991) [7], which therefore were also implemented in VieVS. Processing the data with the three models showed good agreement, revealing differences in the calculated delay mostly below 1 ps with a few exceptions up to 3 ps. These correspond to the theoretical differences of the models, as given in the literature mentioned above.

2.1. Results

The quality of our delay modeling can be expressed by the agreement between the computed (theoretical) delay and the measured one. In other words, we simply look at the observed-minus-computed (o-c) values. Before the observed values are used, they are corrected for ambiguities and additionally one offset per baseline is estimated for each continuous observation period. For the analyzed data, the o-c values are mostly at a level of ±10 mm (30 ps), as shown in Figure 1. Thus, our results largely agree with those published by NAOJ Mizusawa [5]. In the figure, each color represents one baseline; long time periods without observations were excluded for clarity (dashed vertical lines). It can be clearly seen that there is some signal left in the data without a fully identified origin. In Sections 2.2 and 2.3 we try to assess further error sources and investigate the extent to which they might contribute to these remaining signals.

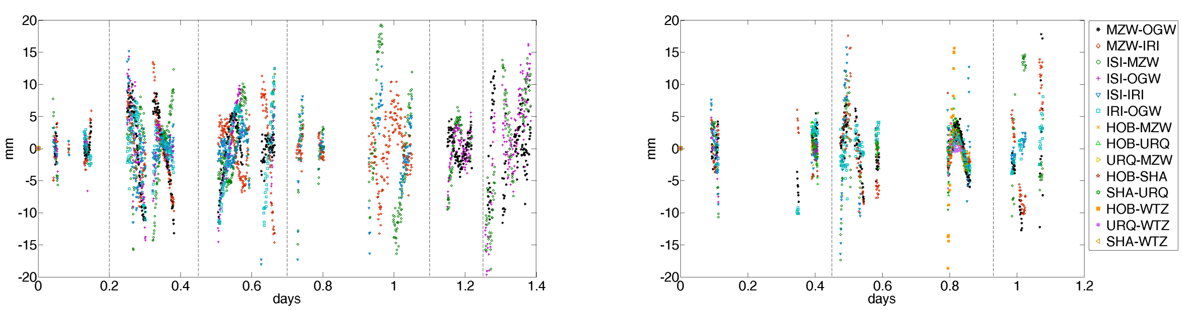

October 2008 January 2008

Figure 1. Observed-minus-computed values.

2.2. Level of Cancellation

The strength of D-VLBI observations is the high level of cancellation. Due to the nearly identical ray path of the signals and the usage of the same antennas at the same time epoch, most of the atmospheric and station dependent delays are the same and cancel out when subtracting the two sources. Table 1 gives an overview of different effects, their magnitude in the single delay to one source (τ), and the size of the residual effect in $\Delta\tau$. The given values represent the empirically determined maxima of the processed data. Because of the key role of the observation network in this investigation, we treated the much longer intercontinental baselines separately; these values are given in brackets. Clearly visible is the fact that with the remaining signals <10 ps (3 mm), geometric effects are almost totally canceled out and can be ignored for the following studies. This is not the case for the atmosphere. In general we can say that the values vary much more; this is due to its strong dependency on the elevation angle of the observations. Most of the processed observations were taken at elevations >20°, but for some of the long baselines elevation angles of 10° or even 5° were found. The biggest part comes from the hydrostatic part of the troposphere. Here we assume that this effect can be modeled in the VLBI analysis software rather well.

Table 1. Level of cancellation in D-VLBI observations $\Delta\tau$ compared to the total effect in τ.

(values in brackets represent long baselines)	τ	$\Delta\tau$
GEOMETRY		
Antenna ±5 cm	300 ps	1-2 ps
Orbit ±10 m	150-1000 ps	2-8 ps
EOP	5 (60) ps	< 0.05 (0.1) ps
dUT1: 5 ms/xp,yp: 200 mas		
dX,dY: 300 mas		
ATMOSPHERE		
Hydrostatic troposphere, a priori	2-20 (10-60) ns	30-300 (50-1000) ps
Wet troposphere, ECMWF	1-3 (4) ns	4-40 (10-60) ps
Ionosphere, TEC-maps	1.5 (2-10) ns	10 (80) ps

2.3. Further Effects

So far, the **wet troposphere** is not included in our processing. In order to estimate its scale, the values in Table 1 were calculated using numerical weather model data from the European Centre for Medium-Range Weather Forecast (ECMWF) as available with the Vienna Mapping Functions (VMF) [2]. Due to the narrow separation angle of the observations, this effect reduces to several picoseconds and might only influence the o-c critically on the intercontinental baselines when observations at very low elevations are performed. The effect of the **ionosphere** was determined by using GNSS-derived maps of the total electron content (TEC). In Figure 2 the results for the October data are plotted, also serving as a typical example for the connection of the systematics in the results with the separation angles (gray areas in the back) and with the four elevation angles from the two antennas to the two sources (brownish colors). Its values appear to be unusually small, because most of the observations were performed during the night when the ionosphere is rather inactive. Using the simulation tool in VieVS, we estimated the effect of **atmospheric**

turbulence on the calculated delay. Details about the simulation method can be found in [9]. The results again show strong dependency on the separation and elevation angle, having values of some picoseconds with extremes up to 30-40 ps. As these results are based on Monte Carlo simulations as well as on some assumptions about the atmospheric behavior, the results cannot be quantified straightforwardly.

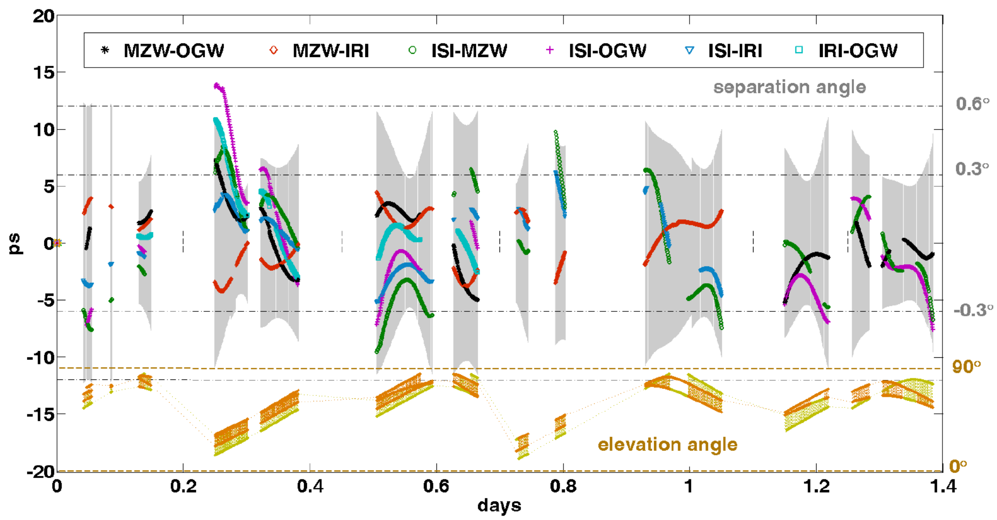

Figure 2. Residual ionosphere per baseline (October data). Additionally, the elevation and separation angles are plotted.

In summary we can say that some further effects of the atmosphere clearly reach the level of significance. Nevertheless, when applied in the processing, the residual signals diminished for certain time epochs and baselines, but it increased for others.

3. Orbit Estimation

As the SELENE D-VLBI observations were done to support the orbit determination of the transmitting sources, we implemented the orbit estimation in VieVS. Following equation (1), the derivative of the differenced phase delay with respect to the relative source position of Vstar to Rstar yields:

$$\frac{\partial \Delta\tau}{\partial X_V} = -\frac{X_V - X_1}{r_{V1}} + \frac{X_V - X_2}{r_{V2}}. \tag{2}$$

X denotes the position of Vstar (V) and of the antenna at station i, in the denominator the distance r_{Vi} from Vstar to the i-th antenna is found. In principle, applying this formula for Cartesian coordinates is easy; nevertheless due to the weak geometry the unknowns (e.g., Δxyz) are highly correlated, causing the estimation process to be unstable. For the investigated dataset, residuals of some kilometers appear. A possible way to address this problem is to constrain the absolute distance in the direction of the line of sight and only allow movement perpendicular to it. Following this approach, the residuals could be reduced to some meters. This is a reasonable result, as the NAOJ determined the total orbit errors to be at an average level of 18 m [4].

4. Conclusions

We showed our experiences with the processing of SELENE D-VLBI data in VieVS. The implementation in the existing VieVS software was realized, and the results are equivalent to the comparable values of NAOJ. Further, a table with the level of cancellation for various geometric and atmospheric contributors to the measured time delay was given. While the geometric effects can be neglected, some atmospheric aspects are more critical and were discussed in more depth. For orbit estimation we recommend introducing constraints during estimation or adequate weighting and combination with other measurements.

Acknowledgements

The authors want to thank NAOJ Mizusawa for providing the data. Parts of the work described in this contribution were done within the projects VLBI-ART (P24187-N21), GGOS Atmosphere (P20902-N10) by the Austrian Science Fund (FWF), and D-VLBI of the DFG Research Unit on reference systems (FOR1503).

References

[1] Böhm, J., S. Böhm, T. Nilsson, A. Pany, L. Plank, H. Spicakova, K. Teke, H. Schuh, The new Vienna VLBI Software VieVS, In: Proceedings of IAG Scientific Assembly 2009, International Association of Geodsy Symposia Series Vol. 136, edited by S. Kenyon, M. C. Pacino, and U. Marti, 1007-1011, 2012, doi: 10.1007/978-3-642-20338-1-126.

[2] Böhm, J., B. Werl, and H. Schuh, Troposphere mapping functions for GPS and very long baseline interferometry from European Centre for Medium-Range Weather Forecasts operational analysis data, J. Geophys. Res., 111, B02406, 2006 doi:10.1029/2005JB003629.

[3] Fukushima, T., Lunar VLBI observation model, Astronomy and Astrophysics, 291, pp 320-323, 1994.

[4] Goossens, S., K. Matsumoto, D. D. Rowlands, F. G. Lemoine, H. Noda, H. Araki, Orbit determination of the SELENE satellites using multi-satellite data types and evaluation of SELENE gravity field models, Journal of Geodesy, 85, 487-504, Springer-Verlag, 2011, doi:10.1007/s00190-011-0449-2.

[5] Goossens, S. et al., Lunar gravity field determination using SELENE same-beam differential VLBI tracking data, Journal of Geodesy, Springer-Verlag, 2010, doi:10.1007/s00190-010-0430-2.

[6] Kikuchi, F. et al., Picosecond accuracy VLBI of the two subsatellites of SELENE (KAGUYA) using multifrequency and same beam methods, Radio Science, 44, RS2008, 2009, doi:10.1029/2008RS003997.

[7] Klioner, S. A., General Relativistic Model of VLBI Observables, In: Carter W. E. (ed), Proceedings of the AGU Chapman Conference on Geodetic VLBI: Monitoring Global Change, NOAA Technical Report NOS 137 NGS 49, American Geophysical Union, Washington, D. C., pp 188-202, 1991.

[8] Liu, Q. et al., Same-beam VLBI observations of SELENE for improving lunar gravity field model, Radio Science, Vol. 45, RS2004, 2010, doi:10.1029/2009RS004203.

[9] Pany, A., J. Böhm, D. MacMillan, H. Schuh, T. Nilsson, J. Wresnik, Monte Carlo simulations of the impact of troposphere, clock and measurement errors on the repeatability of VLBI positions, Journal of Geodesy, 85, pp. 39-50, 2011, doi: 10.1007/s00190-010-0415-1.

[10] Sekido, M. and T. Fukushima, A VLBI delay model for radio sources at a finite distance, Journal of Geodesy, 80, pp 137-149, 2006, doi:10.1007/s00190-006-0035-y.